Article

Cell Reports

ATP-Citrate Lyase Controls a Glucose-to-Acetate Metabolic Switch

Graphical Abstract

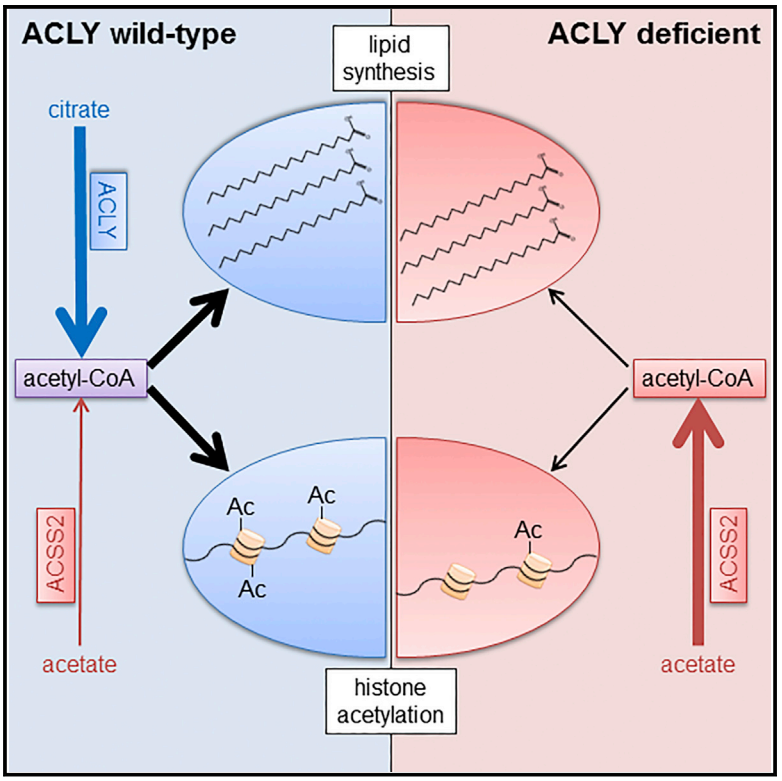

Authors

Steven Zhao, AnnMarie Torres, Ryan A. Henry, ..., Nathaniel W. Snyder, Andrew J. Andrews, Kathryn E. Wellen

Correspondence

wellenk@exchange.upenn.edu

In Brief

Zhao et al. demonstrate that ACLY deficiency causes upregulation of ACSS2 in proliferating cells in vitro and adipocytes in vivo. Acetate is needed for viability and is used for lipid synthesis and histone acetylation in the absence of ACLY. Proliferation is constrained in ACLY-deficient cells, despite ACSS2 compensation.

Highlights

- ACSS2 is upregulated upon genetic deletion of *Acly* in vitro and in vivo
- Acetate sustains viability in *Acly*-deficient MEFs, but proliferation is impaired
- Low levels of acetate can supply abundant acetyl-CoA in the absence of ACLY
- Acetate partially rescues lipogenesis and histone acetylation in ACLY deficiency

Zhao et al., 2016, Cell Reports *17*, 1037–1052
October 18, 2016
http://dx.doi.org/10.1016/j.celrep.2016.09.069

Cell Reports
Article

ATP-Citrate Lyase Controls a Glucose-to-Acetate Metabolic Switch

Steven Zhao,[1,2,7] AnnMarie Torres,[1,2,7] Ryan A. Henry,[5] Sophie Trefely,[1,2,4] Martina Wallace,[6] Joyce V. Lee,[1,2] Alessandro Carrer,[1,2] Arjun Sengupta,[3] Sydney L. Campbell,[1,2] Yin-Ming Kuo,[5] Alexander J. Frey,[4] Noah Meurs,[6] John M. Viola,[1,2] Ian A. Blair,[3] Aalim M. Weljie,[3] Christian M. Metallo,[6] Nathaniel W. Snyder,[4] Andrew J. Andrews,[5] and Kathryn E. Wellen[1,2,8,*]

[1]Department of Cancer Biology
[2]Abramson Family Cancer Research Institute
[3]Department of Systems Pharmacology and Translational Therapeutics
Perelman School of Medicine, University of Pennsylvania, Philadelphia, PA 19104, USA
[4]A.J. Drexel Autism Institute, Drexel University, Philadelphia, PA 19104, USA
[5]Department of Cancer Biology, Fox Chase Cancer Center, Philadelphia, PA 19111, USA
[6]Department of Bioengineering and Institute of Engineering in Medicine, University of California, San Diego, La Jolla, CA 92093, USA
[7]Co-first author
[8]Lead Contact
*Correspondence: wellenk@exchange.upenn.edu
http://dx.doi.org/10.1016/j.celrep.2016.09.069

SUMMARY

Mechanisms of metabolic flexibility enable cells to survive under stressful conditions and can thwart therapeutic responses. Acetyl-coenzyme A (CoA) plays central roles in energy production, lipid metabolism, and epigenomic modifications. Here, we show that, upon genetic deletion of *Acly*, the gene coding for ATP-citrate lyase (ACLY), cells remain viable and proliferate, although at an impaired rate. In the absence of ACLY, cells upregulate ACSS2 and utilize exogenous acetate to provide acetyl-CoA for de novo lipogenesis (DNL) and histone acetylation. A physiological level of acetate is sufficient for cell viability and abundant acetyl-CoA production, although histone acetylation levels remain low in ACLY-deficient cells unless supplemented with high levels of acetate. ACLY-deficient adipocytes accumulate lipid in vivo, exhibit increased acetyl-CoA and malonyl-CoA production from acetate, and display some differences in fatty acid content and synthesis. Together, these data indicate that engagement of acetate metabolism is a crucial, although partial, mechanism of compensation for ACLY deficiency.

INTRODUCTION

Acetyl-coenzyme A (CoA) is a central molecule in cell metabolism, signaling, and epigenetics. It serves crucial roles in energy production, macromolecular biosynthesis, and protein modification (Carrer and Wellen, 2015; Pietrocola et al., 2015). Within mitochondria, acetyl-CoA is generated from pyruvate by the pyruvate dehydrogenase complex (PDC), as well as from catabolism of fatty acids and amino acids. To enter the tricarboxylic acid (TCA) cycle, acetyl-CoA condenses with oxaloacetate, producing citrate, a reaction catalyzed by citrate synthase. Transfer of acetyl-CoA from mitochondria to the cytosol and nucleus involves the export of citrate and its subsequent cleavage by ATP-citrate lyase (ACLY), generating acetyl-CoA and oxaloacetate. This acetyl-CoA is used for a number of important metabolic functions, including synthesis of fatty acids, cholesterol, and nucleotide sugars such as UDP-N-acetylglucosamine. Acetyl-CoA also serves as the acetyl-group donor for both lysine and N-terminal acetylation (Carrer and Wellen, 2015; Pietrocola et al., 2015). ACLY plays an important role in regulating histone acetylation levels in diverse mammalian cell types (Covarrubias et al., 2016; Donohoe et al., 2012; Lee et al., 2014; Wellen et al., 2009).

In addition to ACLY, nuclear-cytosolic acetyl-CoA is produced from acetate by acyl-CoA synthetase short chain family member 2 (ACSS2) (Luong et al., 2000). Recent studies have revealed an important role for this enzyme in hypoxia and in some cancers (Comerford et al., 2014; Gao et al., 2016; Kamphorst et al., 2014; Mashimo et al., 2014; Schug et al., 2015, 2016; Yoshii et al., 2009). Acetate can be produced intracellularly by histone deacetylase reactions or can be imported from the environment (Carrer and Wellen, 2015). Levels of acetate in circulating blood are rather low, ranging from 50 to 200 μM in humans, although acetate concentrations can increase substantially in certain conditions, such as following alcohol consumption, high-fat feeding, or infection, or in specific locations such as the portal vein (Balmer et al., 2016; Herrmann et al., 1985; Lundquist et al., 1962; Perry et al., 2016; Scheppach et al., 1991; Skutches et al., 1979; Tollinger et al., 1979). Acetate is also exported by cells under certain conditions, such as low intracellular pH (McBrian et al., 2013), and thus could potentially be made available for uptake by other cells in the immediate microenvironment. Two additional acetyl-CoA-producing enzymes, the

PDC and carnitine acetyltransferase (CrAT), have been reported to be present in the nucleus and to contribute acetyl-CoA for histone acetylation (Madiraju et al., 2009; Sutendra et al., 2014). The PDC was shown to translocate from mitochondria to the nucleus under certain conditions, such as growth factor stimulation; within the nucleus, the complex is intact and retains the ability to convert pyruvate to acetyl-CoA (Sutendra et al., 2014). The relative contributions of each of these enzymes to the regulation of histone acetylation and lipid synthesis, as well as the mechanisms of metabolic flexibility between these enzymes, are poorly understood.

Whole-body loss of ACLY is early embryonic lethal, indicating that it serves non-redundant roles during development (Beigneux et al., 2004). Silencing or inhibition of ACLY suppresses the proliferation of many cancer cell lines and impairs tumor growth (Bauer et al., 2005; Hanai et al., 2012; Hatzivassiliou et al., 2005; Migita et al., 2008; Shah et al., 2016; Zaidi et al., 2012). Depending on the context, ACLY silencing or inhibition can also promote senescence (Lee et al., 2015), induce differentiation (Hatzivassiliou et al., 2005), or suppress cancer stemness (Hanai et al., 2013), further pointing to its potential as a target for cancer therapy. Inhibition of ACLY in adult animals and humans is reasonably well tolerated and produces blood lipid-lowering effects (Ballantyne et al., 2013; Gutierrez et al., 2014; Pearce et al., 1998). Thus, there may be a therapeutic window for ACLY inhibition in treatment of cancer and/or metabolic diseases; although the extent to which cells could leverage other compensatory mechanisms upon reduced ACLY function is not clear.

In this study, we aimed to elucidate two questions: first, does use of glucose-derived carbon for fatty acid synthesis and histone acetylation require ACLY; and second, can cells compensate for ACLY deficiency and, if so, by which mechanisms or pathways? To address these questions, we generated a conditional mouse model of *Acly* deficiency (*Acly*$^{f/f}$ mice), as well as immortalized mouse embryonic fibroblast (MEF) cell lines (*Acly*$^{f/f}$ MEFs). As a complement to these models, we used CRISPR-Cas9 genome editing to delete *ACLY* from human glioblastoma cells. ACLY deficiency in both MEFs and glioblastoma cells potently impaired proliferation and suppressed histone acetylation levels. Both lipid synthesis and histone acetylation from glucose-derived carbon were severely impaired in ACLY-deficient MEFs. Cells partially compensated for the absence of ACLY by upregulating ACSS2, and ACLY-deficient MEFs became dependent on exogenous acetate for viability. Acetate was used to supply acetyl-CoA for both lipid synthesis and histone acetylation, although global histone acetylation levels remained low unless cells were supplemented with high levels of acetate. ACSS2 upregulation in the absence of ACLY was also observed in vivo upon deletion of *Acly* from adipocytes in mice. *Acly*$^{FAT-/-}$ mice exhibited normal body weight and adipose tissue architecture, and production of acetyl-CoA and malonyl-CoA from acetate was enhanced in ACLY-deficient adipocytes. Upon deuterated-water (D_2O) labeling of wild-type (WT) and *Acly*$^{FAT-/-}$ mice, we observed that de novo synthesized fatty acids were present in white adipose tissue (WAT) in both genotypes, although some differences between depots were apparent. Visceral (epididymal) WAT (VWAT) exhibited no significant differences between WT and *Acly*$^{FAT-/-}$ mice in quantities of de novo synthesized fatty acids, while synthesized saturated fatty acids were reduced in subcutaneous (inguinal) WAT (SWAT) of *Acly*$^{FAT-/-}$ mice. Histone acetylation levels were also significantly altered in *Acly*$^{FAT-/-}$ SWAT. Taken together, this study demonstrates that ACLY is required for glucose-dependent fatty acid synthesis and histone acetylation and that a major, albeit partial, compensatory mechanism for ACLY deficiency involves engagement of acetate metabolism.

RESULTS

Genetic Deletion of *Acly* in Cells Is Consistent with Viability but Impairs Proliferation

To facilitate investigation of the role of ACLY in vitro and in vivo, we generated a conditional mouse model of *Acly* deficiency, using a conventional Cre-lox strategy (*Acly*$^{f/f}$ mice) (Figure S1A). MEFs from *Acly*$^{f/f}$ mice were immortalized (*Acly*$^{f/f}$ MEFs). *Acly* was efficiently deleted from *Acly*$^{f/f}$ MEFs upon administration of Cre recombinase (Figure S1B). *Acly*$^{\Delta/\Delta}$ MEFs continued to proliferate, although more slowly than parental cells (Figure S1C). However, over time, these cells regained ACLY expression, indicating that deletion occurred in less than 100% of cells and that those that retained ACLY had a growth advantage over *Acly*$^{\Delta/\Delta}$ cells (Figure S1B). To address this, we generated three clonal *Acly* knockout (KO) cell lines, designated PC7, PC8, and PC9 (Figure 1A). ACSS2 was strikingly upregulated in these cell lines (Figure 1A). Proliferation in the absence of ACLY was significantly slower in each of the KO cell lines than in the parental *Acly*$^{f/f}$ cells (Figure 1B). We also used CRISPR-Cas9 to delete *ACLY* from LN229 glioblastoma cells (Figure 1C). ACSS2 levels were high at baseline in LN229 cells and only modestly increased with *ACLY* deletion (Figure 1C). However, similar to the ACLY-deficient MEFs, ACLY-deficient LN229 clones exhibited a marked proliferative impairment (Figure 1D).

Two of the ACLY-KO clones, PC7 and PC9, were reconstituted with wild-type ACLY (ACLY-WT) or a catalytically inactive ACLY mutant (ACLY-H760A) (Figures 1E and S1D). ACLY-WT, but not ACLY-H760A, significantly restored proliferation in the KO clones (Figures 1F and S1E). Of note, despite comparable expression upon initial reconstitution (data not shown), ACLY-H760A failed to stably express as highly as ACLY-WT (Figure S1D), further pointing to a strong selective advantage for cells expressing catalytically active ACLY. ACSS2 levels were elevated in both the nucleus and cytoplasm of ACLY-deficient cells, and this was reversed upon reconstitution of ACLY-WT (Figure 1E).

Next, we inquired whether ACSS2 upregulation was induced by ACLY deletion or whether growing up ACLY-deficient clones selected for those that already had high ACSS2 expression. To test this, we examined the timing of ACSS2 upregulation upon loss of ACLY function. In *Acly*$^{f/f}$ MEFs, ACSS2 was rapidly upregulated in parallel to loss of ACLY protein following Cre administration (Figure 1G). Moreover, treatment of MEFs with an ACLY inhibitor (BMS-303141) led to increased ACSS2 within 96 hr

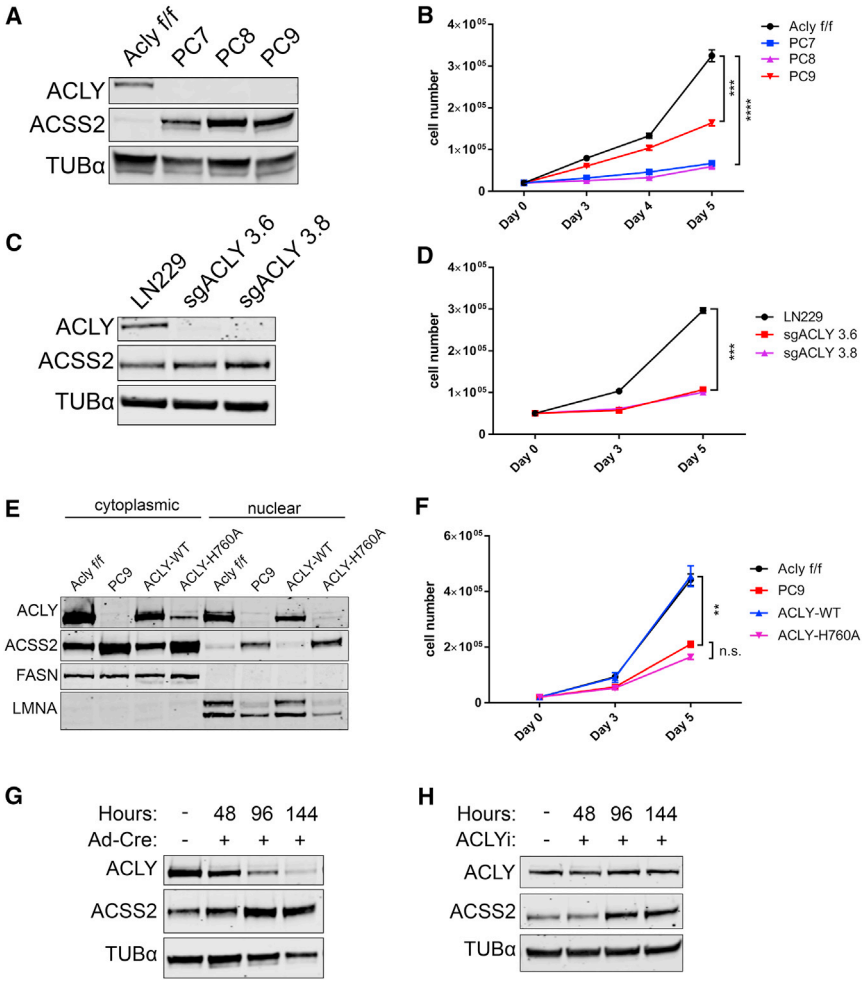

Figure 1. Genetic Deletion of *Acly* Is Consistent with Cell Viability but Impairs Proliferation

(A) Western blot of three clonal ACLY-deficient (KO) cell lines (PC7, PC8, and PC9) generated from *Acly*$^{f/f}$ MEFs.

(B) Proliferation curve of *Acly*$^{f/f}$ and ACLY-KO MEFs over 5 days; mean ± SEM of triplicate wells, statistical significance compared to *Acly*$^{f/f}$.

(C) Western blot verification of *ACLY* knockout by CRISPR-Cas9 in LN229 glioblastoma cells.

(D) Proliferation curve of LN229 and two ACLY-knockout clonal cell lines over 5 days; error bars indicate mean ± SEM of triplicate wells, statistical significance compared to LN229.

(E) Western blot of nuclear and cytoplasmic fractions of *Acly*$^{f/f}$, PC9, and reconstituted ACLY-WT and ACLY-H760A PC9 cells. FASN and LMNA (lamin A/C) are cytoplasmic and nuclear markers, respectively.

(F) Proliferation curve of *Acly*$^{f/f}$ MEF and PC9 lines compared to PC9 reconstituted with ACLY-WT or ACLY-H760A over 5 days; error bars indicate mean ± SEM of triplicate wells, statistical significance compared to PC9.

(G) Western blot of ACLY and ACSS2 protein levels in *Acly*$^{f/f}$ MEFs over 144 hr following administration of Cre recombinase.

(H) Western blot of ACLY and ACSS2 protein levels in *Acly*$^{f/f}$ MEFs over 144 hr with pharmacological inhibition of ACLY (50 μM BMS-303141).

For all panels: **p < 0.01; ***p < 0.001; ****p < 0.0001; n.s., not significant.

See also Figure S1.

(Figure 1H). Thus, we conclude that the loss of ACLY activity induces ACSS2 upregulation.

ACLY-Deficient MEFs Require Use of Exogenous Acetate for Viability

The amount of acetate in the serum used in these experiments was quantified by nuclear magnetic resonance (NMR). Undiluted calf serum (CS) contained ~800–900 μM acetate, while acetate was undetectable in dialyzed fetal bovine serum (dFBS) (Figures 2A and S2A). Given that acetate was also undetectable in DMEM, our standard culture conditions (DMEM + 10% CS) exposed cells to slightly less than 100 μM acetate. ACLY-deficient cells began to die when cultured in the absence of exogenous acetate (DMEM + 10% dFBS) (Figures 2B–2D), and adding 100 μM acetate was sufficient to restore viability (Figures 2C and 2E). No added proliferative benefit was gained by further increasing the amount of acetate supplemented (Figure 2F). Additionally, reconstitution of ACLY-WT, but not ACLY-H760A, restored the ability of KO cells to grow in acetate-depleted conditions (Figures 2B and 2E). To test whether acetyl-CoA production by ACSS2 was required for viability, we used CRISPR-Cas9 to delete *Acss2* in *Acly*$^{f/f}$ MEFs (Figure S2B). Little to no difference in the proliferation rate was observed upon *Acss2* deletion when *Acly* was intact (Figure S2C). However, subsequent deletion of *Acly* resulted in extensive toxicity (Figures 2G and S2D), which was not observed in cells expressing *Acss2*, confirming that cells rely on ACSS2 for survival in the absence of ACLY.

Physiological Levels of Acetate Support Lipid Synthesis in the Absence of ACLY

ACLY deficiency did not alter rates of glucose or glutamine consumption, although lactate and glutamate production were elevated (Figure 3A). To confirm the requirement for ACLY for glucose-dependent fatty acid synthesis and test the use of acetate, we set up parallel stable isotope tracer experiments in which *Acly*$^{f/f}$, PC9, PC9-ACLY-WT, and PC9-ACLY-H760A cells were incubated for 48 hr either with [U-^{13}C]glucose (10 mM) and unlabeled acetate (100 μM) or with [1,2-^{13}C]acetate (100 μM) and unlabeled glucose (10 mM) (Figure 3B). In ACLY-proficient cells, palmitate was strongly labeled from glucose-derived carbon, as expected. In PC9 ACLY-KO cells, labeling of palmitate from ^{13}C-glucose was nearly abolished; this could be restored by reconstitution of ACLY-WT but not ACLY-H760A (Figure 3C). Conversely, a marked increase in use of acetate for fatty acid synthesis was observed in PC9 and PC9-ACLY-H760A cells

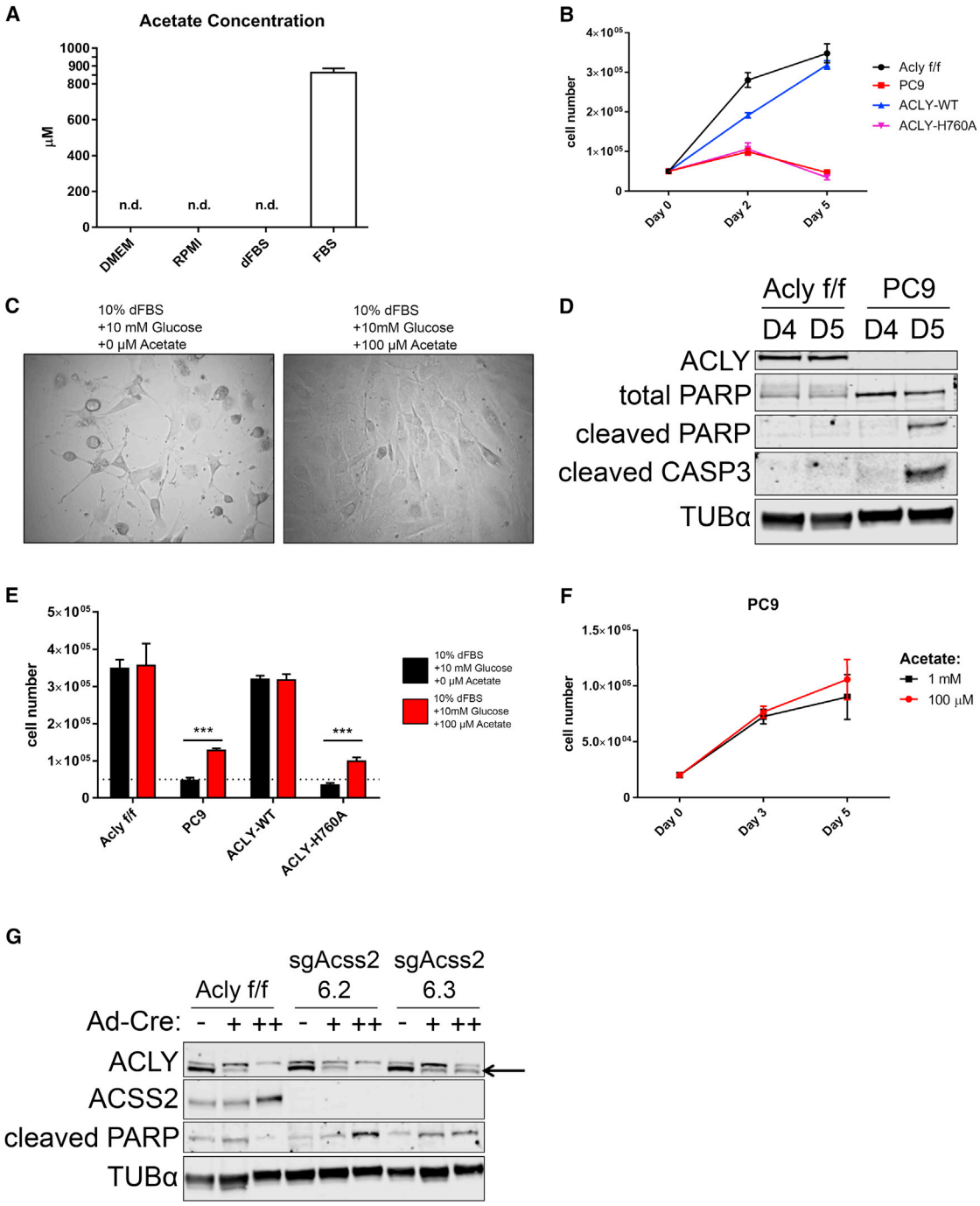

Figure 2. ACLY-Deficient MEFs Require Exogenous Acetate for Viability

(A) Acetate concentrations in DMEM, RPMI, 100% dialyzed fetal bovine serum (dFBS), and 100% calf serum (CS); error bars indicate mean ± SEM of triplicate aliquots. See Figure S2A for spectrum. n.d., not detected.

(B) Proliferation curve over 5 days of *Acly*$^{f/f}$, PC9, PC9-ACLY-WT, and PC9-ACLY-H760A cells in acetate-free conditions (DMEM + 10% dFBS + 10 mM glucose); error bars indicate mean ± SEM of triplicate wells.

(C) Image of ACLY-deficient PC9 cells cultured for 5 days in DMEM + 10% dFBS + 10 mM glucose, without (left) or with (right) 100 µM sodium acetate.

(D) Western blot of apoptotic markers cleaved poly(ADP-ribose) polymerase (PARP) and cleaved caspase-3 (CASP3) in *Acly*$^{f/f}$ and PC9 cells cultured in acetate-free conditions (DMEM + 10% dFBS + 10 mM glucose) for 4 (D4) or 5 (D5) days.

(E) Cell numbers following 5 days in culture in DMEM + 10% dFBS + 10 mM glucose alone (black) or supplemented with 100 µM sodium acetate (red) in *Acly*$^{f/f}$, PC9, PC9-ACLY-WT, and PC9-ACLY-H760A cells; error bars indicate mean ± SEM of triplicates. ***p < 0.001. Dotted line represents cell number at plating.

(legend continued on next page)

(Figure 3D). We also examined the use of glucose and acetate carbon for synthesis of HMG (hydroxymethylglutaryl)-CoA, an intermediate in the mevalonate pathway and ketone body synthesis. Again, parental and PC9-ACLY-WT cells used glucose-derived carbon for HMG-CoA synthesis (Figure 3E). In the absence of ACLY, glucose carbon use for HMG-CoA synthesis was extremely limited (Figure 3E); instead, acetate was used (Figure 3F). Total levels of HMG-CoA trended slightly lower in the PC9 cells, though this difference was not statistically significant (Figure 3G). The data thus show that, in MEFs, glucose-dependent synthesis of fatty acids and HMG-CoA is nearly completely dependent on ACLY, and a physiological level of acetate can at least partially support lipid synthesis in its absence.

ACLY Is the Primary Supplier of Acetyl-CoA for Maintaining Global Histone Acetylation

Histone acetylation is another major fate of nuclear-cytosolic acetyl-CoA. Consistent with previous data using RNAi-mediated ACLY silencing (Lee et al., 2014; Wellen et al., 2009), global levels of histone acetylation were strikingly reduced upon genetic deletion of *Acly*, despite increased ACSS2. Moreover, although 100 μM acetate was sufficient to restore survival in dFBS-cultured KO cells, it failed to rescue histone acetylation levels. However, incubating cells with a high level of acetate (1 mM) markedly increased histone acetylation levels in KO cells (Figure 4A). Reciprocally, histone acetylation levels were low in WT MEFs when cultured in 1 mM glucose and increased with greater glucose concentrations. In KO cells, histone acetylation levels were low at all concentrations of glucose tested, up to 25 mM (Figure S3A). Reconstitution of PC9 cells with ACLY-WT but not, ACLY-H760A, restored histone acetylation levels to those in the parental cells (Figure 4A).

To determine the respective use of glucose- and acetate-derived carbon for histone acetylation in each of the MEF cell lines, we conducted stable isotope tracer experiments under three conditions: (1) [U-^{13}C]glucose (10 mM) and unlabeled acetate (100 μM), (2) physiological [1,2-^{13}C]acetate (100 μM) and unlabeled glucose (10 mM), or (3) high [1,2-^{13}C]acetate (1 mM) and unlabeled glucose (10 mM) (Figure S3B). In condition 1, histone acetyl groups were strongly labeled from ^{13}C-glucose in *Acly*$^{f/f}$ and PC9-ACLY-WT cells (Figures 4B, 4E, and S3C). In PC9 and PC9-ACLY-H760A cells, labeling of histone acetyl groups from glucose carbon was severely compromised (Figures 4B, 4E, and S3C). Moreover, aligning with western blot data, total levels of histone acetylation were lower in cells lacking functional ACLY (Figure 4E). Thus, the data indicate that ACLY is required for the majority of glucose-dependent histone acetylation. In cells lacking functional ACLY (PC9 and PC9-ACLY-H760A), 100 μM acetate contributed carbon to histone acetylation with ~40%–60% of the acetyl groups derived from acetate after 24-hr labeling (Figure 4C), but total acetylation remained low (Figures 4F and S3D). In 1 mM ^{13}C-acetate, total histone acetylation levels rose (Figures 4G and S3E), consistent with western blot data, and acetate carbon constituted the majority of histone acetyl groups (Figure 4D). These data indicate that ACLY is the dominant supplier of acetyl-CoA for histone acetylation in standard, nutrient-rich conditions and that, in its absence, cells can use acetate to supply acetyl-CoA for histone acetylation, although high exogenous acetate availability is needed to bring histone acetylation up to levels matching those of ACLY-proficient cells. Of note, high acetate did not produce a corresponding rescue of proliferation (Figure 2F). Thus, while ACLY-deficient cells exhibit both slower proliferation and lower histone acetylation levels, histone acetylation can be raised with high acetate without restoration of normal rates of proliferation, supporting the notion that metabolism regulates histone acetylation at least partially independently of proliferation.

We previously defined acetyl-CoA-responsive gene sets in LN229 glioblastoma cells (Lee et al., 2014). Cell-cycle- and DNA-replication-related genes were enriched among those genes that were suppressed in low glucose and increased by both glucose and acetate, although only glucose impacted doubling time (Lee et al., 2014). As observed in MEFs, ACLY deletion in LN229 cells abolished glucose-dependent regulation of global histone acetylation (Figure S4A). Acetate supplementation increased histone acetylation in ACLY null LN229 cells in a dose-dependent manner (Figure S4A). Consistently, the ability of glucose to promote expression of proliferation-related genes (*E2F2*, *MCM10*, and *SKP2*) was potently inhibited in ACLY-deficient cells. Expression of these genes exhibited dose-dependent rescue by acetate (Figure S4B), correlating with global histone acetylation levels, despite the lack of a proliferation rescue (Figure S4C). In addition, we were surprised to find that whole-cell acetyl-CoA levels were minimally impacted in ACLY-KO as compared to WT LN299 cells in high-glucose conditions (Figure S4D).

Acetyl-CoA Levels Are Maintained by Acetate in ACLY-Deficient Cells

In prior studies, global histone acetylation levels have tracked closely with cellular acetyl-CoA levels (Cai et al., 2011; Cluntun et al., 2015; Lee et al., 2014). It was, therefore, unexpected to find these uncoupled in ACLY-KO LN229 cells (Figure S4D). We further explored this in ACLY-KO MEFs and found that acetyl-CoA levels were significantly higher in the KO cells than in the WT *Acly*$^{f/f}$ cells when cultured in 10 mM glucose and 100 μM acetate (Figure 5A). These data suggested either that mitochondrial acetyl-CoA, which is inaccessible for histone acetylation (Takahashi et al., 2006), is elevated in ACLY-KO cells or that ACSS2 compensation allows plentiful nuclear-cytosolic acetyl-CoA production from acetate but that this acetate-derived acetyl-CoA is used less effectively than glucose-derived acetyl-CoA for histone acetylation. We reasoned that mitochondrial and extra-mitochondrial acetyl-CoA pools in ACLY KO cells

(F) Proliferation of PC9 cells over 5 days cultured in DMEM + 10% dFBS + 10 mM glucose, with 100 μM or 1 mM sodium acetate; error bars indicate mean ± SEM of triplicate wells.

(G) Parental *Acly*$^{f/f}$ MEFs and two clones of ACSS2-deficient *Acly*$^{f/f}$ MEFs were administered Cre recombinase once (+) or twice (++) and proteins collected for western blot after 2 days (+) and 2 weeks (++). See Figure S2D for corresponding images.

See also Figure S2.

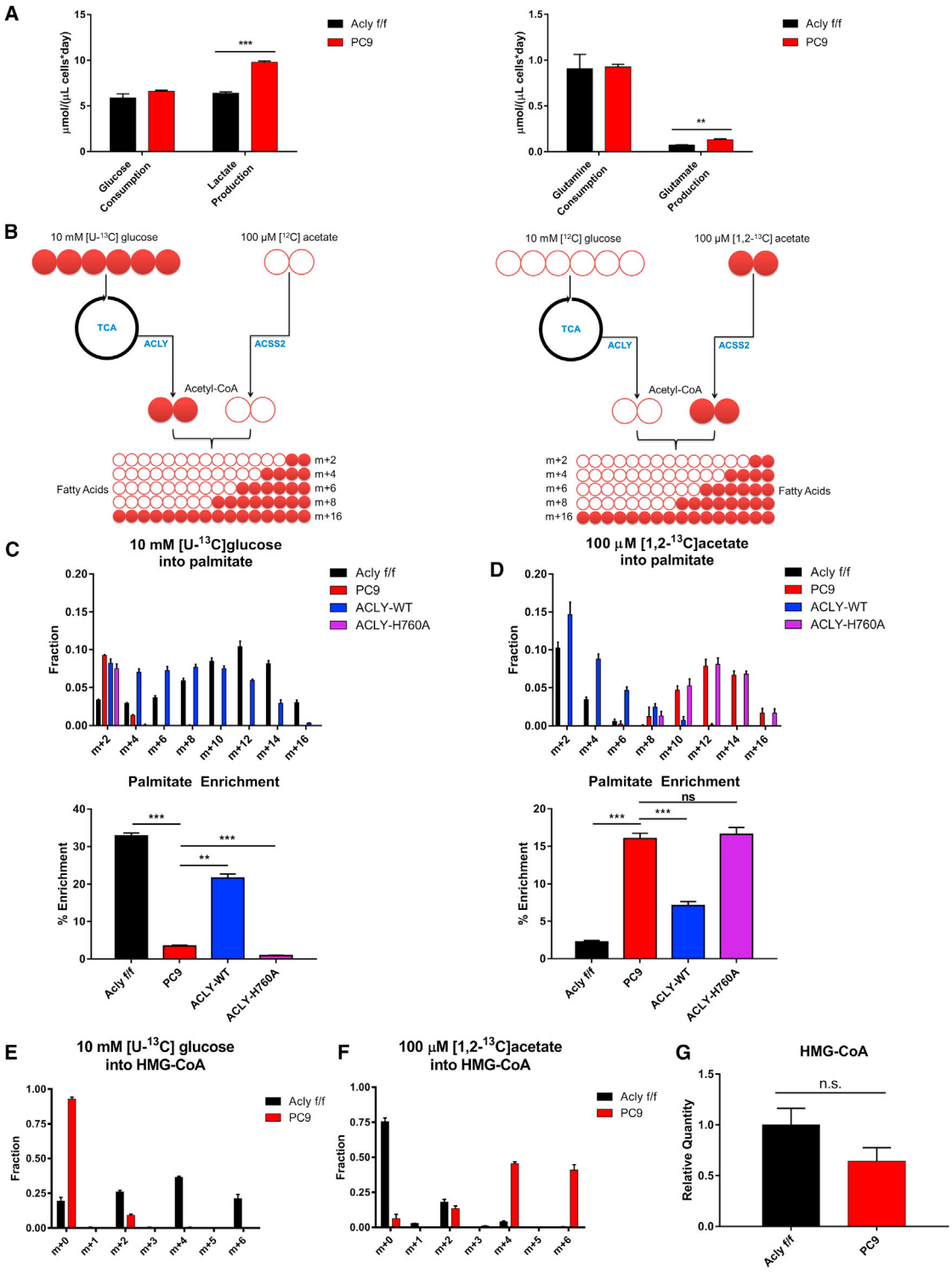

Figure 3. Acetate Supports Lipid Synthesis in the Absence of ACLY

(A) Measurements of glucose consumption and lactate production (left) and glutamine consumption and glutamate production (right), normalized to cell volume (cell number × mean cell volume); error bars indicate mean ± SEM of triplicate wells; **$p < 0.01$; ***$p < 0.001$. Experiment was performed in glucose-free DMEM + 10% dFBS + 10 mM glucose + 100 μM sodium acetate.

(B) Experimental design for heavy isotope labeling of fatty acids using [U-^{13}C]glucose, with unlabeled acetate present (left) and [1,2-^{13}C]acetate, with unlabeled glucose present (right).

(legend continued on next page)

could be distinguished based on whether whole-cell acetyl-CoA is derived from glucose or from acetate (Figure 5B). This is because, in the absence of ACLY, glucose carbon does not meaningfully contribute to nuclear-cytosolic acetyl-CoA, as determined by its minimal use for either lipid synthesis or histone acetylation (Figures 3 and 4). Within mitochondria, both glucose (via PDC) and acetate (via mitochondrial acetyl-CoA synthetases) can be used to generate acetyl-CoA for citrate synthesis. However, as assessed by enrichment of citrate and malate, acetate contributes minimally to mitochondrial metabolism in both WT and KO cells, while glucose is oxidized in both cell lines under these conditions (albeit to a somewhat lesser extent in KO cells) (Figures 5C, 5D, S5A, and S5B). These data suggest that, in ACLY-KO cells, any glucose-derived acetyl-CoA is mitochondrial, whereas acetate-derived acetyl-CoA is predominantly nuclear cytosolic (Figure 5B). Thus measuring the contribution of glucose and acetate to whole-cell acetyl-CoA should allow us to distinguish whether the increase in acetyl-CoA in ACLY-KO MEFs reflects elevated mitochondrial or extra-mitochondrial acetyl-CoA.

Therefore, we incubated cells with [U-^{13}C]glucose (10 mM) and 100 μM unlabeled acetate or, reciprocally, [1,2-^{13}C]acetate (100 μM) and 10 mM unlabeled glucose. In WT (*Acly*$^{f/f}$) cells, as expected, acetyl-CoA, malonyl-CoA, and succinyl-CoA were more strongly enriched from glucose than acetate (Figures 5E–5G). Interestingly, despite minimal labeling of malonyl-CoA from acetate in WT cells (consistent with palmitate enrichment in Figure 3D), ~20% of the acetyl-CoA pool was enriched from ^{13}C-acetate (Figures 5E and 5F), further hinting at differential partitioning of acetate- and glucose-derived acetyl-CoA. In contrast, in the PC9 ACLY-KO cells, acetyl-CoA was minimally labeled from glucose, and ~80% of the acetyl-CoA pool was labeled from acetate after 6 hr (Figure 5E). Malonyl-CoA, but not succinyl-CoA, was also strongly enriched from ^{13}C-acetate in PC9 cells (Figures 5F and 5G). In sum, these data indicate that acetate is the major source of acetyl-CoA in the absence of ACLY, and it appears to predominantly supply the extra-mitochondrial pool.

A second implication of these data is that, at least in KO cells, the mitochondrial acetyl-CoA pool is likely quite low in comparison to the extra-mitochondrial pool, since acetyl-CoA is minimally labeled from glucose-derived carbon. A large difference in relative acetyl-CoA pool size can explain the apparently paradoxical finding that, in KO cells, citrate is labeled from glucose, despite minimal acetyl-CoA enrichment (Figures 5C and 5E). This interpretation is consistent with findings from a recent study of the mitochondrial metabolome, which found that matrix acetyl-CoA levels are very low unless complex I is inhibited, which increases the NADH/NAD ratio, reducing the activity of citrate synthase (Chen et al., 2016). Notably, another implication of this result is that a much larger nuclear-cytosolic acetyl-CoA pool in cultured cells would explain why whole-cell acetyl-CoA measurements in ACLY-proficient cells correlate closely with histone acetylation levels (Cluntun et al., 2015; Lee et al., 2014).

Together, these data indicate that acetate carbon is used to supply acetyl-CoA for nuclear and cytosolic processes in the absence of ACLY. Nevertheless, histone acetylation levels remain low in the absence of ACLY unless a high level of acetate is supplied, and proliferation remains constrained even in the presence of high acetate. Thus ACSS2 is a key, but partial, mechanism of compensation for ACLY deficiency.

ACSS2 Is Upregulated In Vivo upon Deletion of *Acly* from Adipocytes

Finally, we sought to determine whether ACSS2 is upregulated upon loss of ACLY in vivo. Glucose uptake and glucose-dependent lipid synthesis in adipocytes are closely associated with insulin sensitivity and systemic metabolic homeostasis (Herman and Kahn, 2006; Herman et al., 2012). Moreover, our prior work implicated ACLY in regulating histone acetylation levels and expression of key genes in glucose metabolism, such as *Glut4*, in 3T3-L1 adipocytes (Wellen et al., 2009). To interrogate the role of adipocyte ACLY in vivo, we bred *Acly*$^{f/f}$ mice to *Adiponectin-Cre* transgenic mice, which express Cre specifically in adipocytes (Lee et al., 2013). ACSS2 was upregulated in SWAT and VWAT upon deletion of *Acly* (Figures 6A and 6B). In VWAT, ACSS2 upregulation was more apparent at the protein level than the mRNA level (Figures 6A and 6B). Fatty acid synthase (FASN) protein levels were also elevated in the absence of ACLY, particularly in SWAT (Figure 6A). Lipid droplets formed normally in *Acly*$^{FAT-/-}$ adipocytes; in VWAT, adipocytes were larger than in WT mice, while in SWAT, adipocyte lipid droplet size was comparable between genotypes (Figure 6C). Body weight was indistinguishable between WT and *Acly*$^{Fat-/-}$ mice fed a regular chow diet (Figure 6D). However, overall gene expression patterns were altered, with lower expression of adipocyte genes such as *Glut4* in the *Acly*$^{FAT-/-}$ mice (Figure 6E).

Adipocyte Acetyl-CoA and Lipid Metabolism Is Altered in the Absence of ACLY

These data suggested that acetate metabolism might, at least partially, compensate for ACLY deficiency in adipocytes in vivo. Similar to that observed in MEFs, acetyl-CoA levels were higher

(C) Isotopologue distribution of palmitate after 48-hr labeling in 10 mM [U-^{13}C]glucose in *Acly*$^{f/f}$, PC9, PC9-ACLY-WT, and PC9-ACLY-H760A MEFs (top). Expressed as percent enrichment of palmitate (bottom); error bars indicate mean ± SD of triplicates. **$p < 0.01$; ***$p < 0.001$.
(D) Isotopologues of palmitate after 48-hr labeling in 100 μM [1,2-^{13}C]acetate in *Acly*$^{f/f}$, PC9, PC9-ACLY-WT, PC9-Acly H760A MEFs (top). Expressed as percent enrichment of palmitate (bottom); error bars indicate mean ± SD of triplicates. ***$p < 0.001$; ns, not significant.
(E) Isotopologues of HMG-CoA upon 6-hr labeling in 10 mM [U-^{13}C]glucose (100 μM unlabeled acetate present) in *Acly*$^{f/f}$ and PC9 MEFs; error bars indicate mean ± SD of triplicates.
(F) Isotopologues of HMG-CoA upon 6-hr labeling in 100 μM [1,2-^{13}C]acetate (10 mM unlabeled glucose present) in *Acly*$^{f/f}$ and PC9 MEFs; error bars indicate mean ± SD of triplicates.
(G) Total HMG-CoA quantitation in cells cultured in DMEM + 10% dFBS + 10 mM glucose + 100 μM sodium acetate (unlabeled); error bars indicate mean ± SEM of triplicates. n.s., not significant.

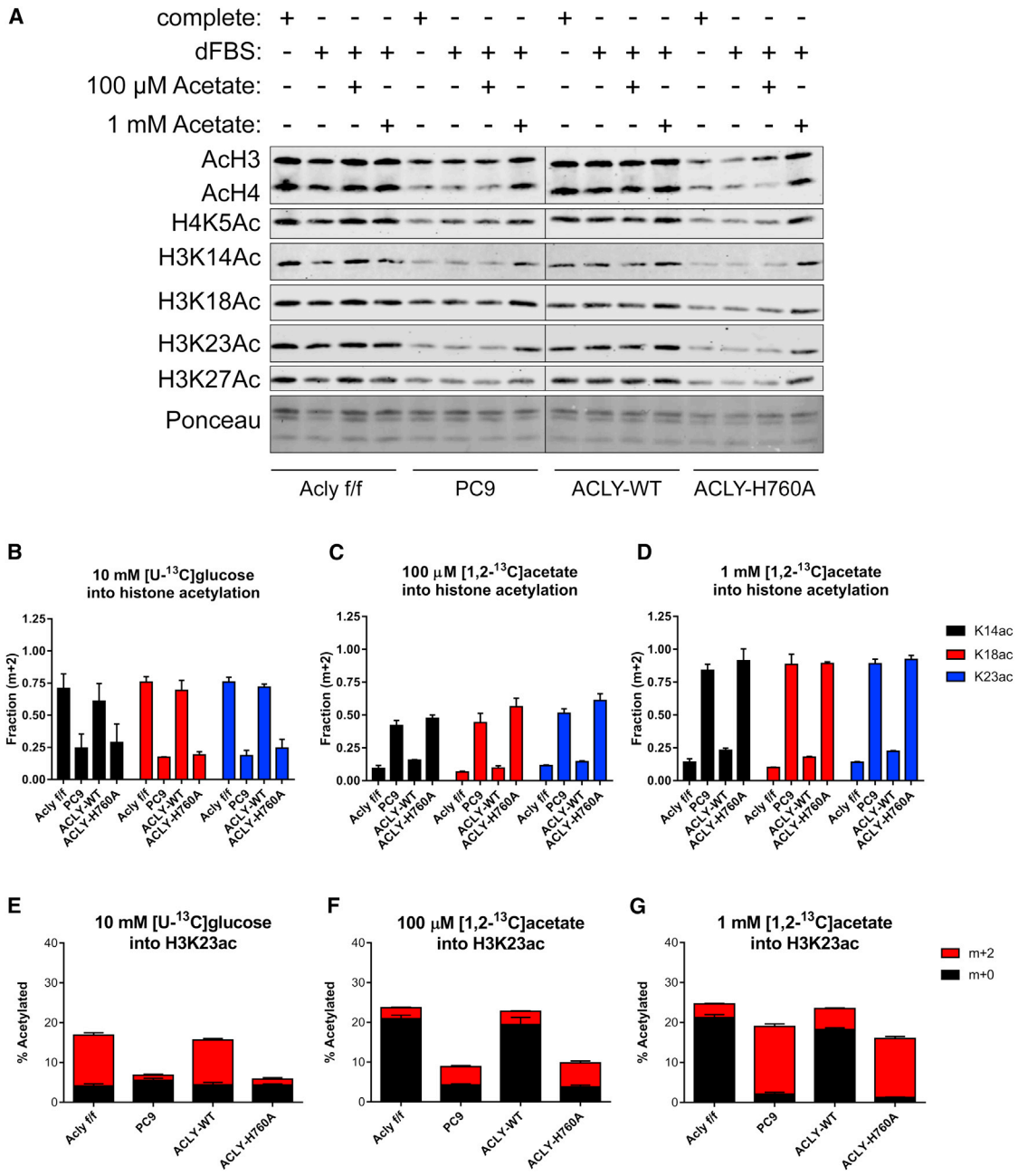

Figure 4. ACLY Is Required for Sustaining Histone Acetylation Levels, despite ACSS2 Compensation

(A) Western blot of acetylated histones extracted from *Acly*$^{f/f}$, PC9, PC9-ACLY-WT, and PC9-ACLY-H760A MEFs cultured in complete medium (DMEM + 10% CS), dFBS medium (DMEM + 10% dFBS), +100 μM acetate medium (DMEM + 10% dFBS + 100 μM sodium acetate), and +1 mM acetate medium (DMEM + 10% dFBS + 1 mM sodium acetate) for 48 hr.

(B–D) Fractions of histone H3-K14, -K18, and -K23 acetylation (m+2) derived from 10 mM [U-^{13}C]glucose, with unlabeled 100 μM acetate present (B); 100 μM [1,2-^{13}C]acetate, with 10 mM unlabeled glucose present (C); or 1 mM [1,2-^{13}C]acetate, with 10 mM unlabeled glucose present (D); error bars indicate mean ± SEM of triplicate samples. Labeling was for 24 hr (see also Figure S3B for experimental design).

(E–G) Overall percentage of H3K23 acetylated in each cell line (y axis), as well as the relative fraction of this acetylation incorporated from a labeled source (red): 10 mM [U-^{13}C]glucose (E), 100 μM [1,2-^{13}C]acetate (F), and 1 mM [1,2-^{13}C]acetate (G) or unlabeled sources (black); error bars indicate mean ± SEM of triplicate samples. The same dataset is represented in parts (B–D) and (E–G). See Figures S3C–S3E for overall percentage data on K14 and K18 acetylation.

See also Figures S3 and S4.

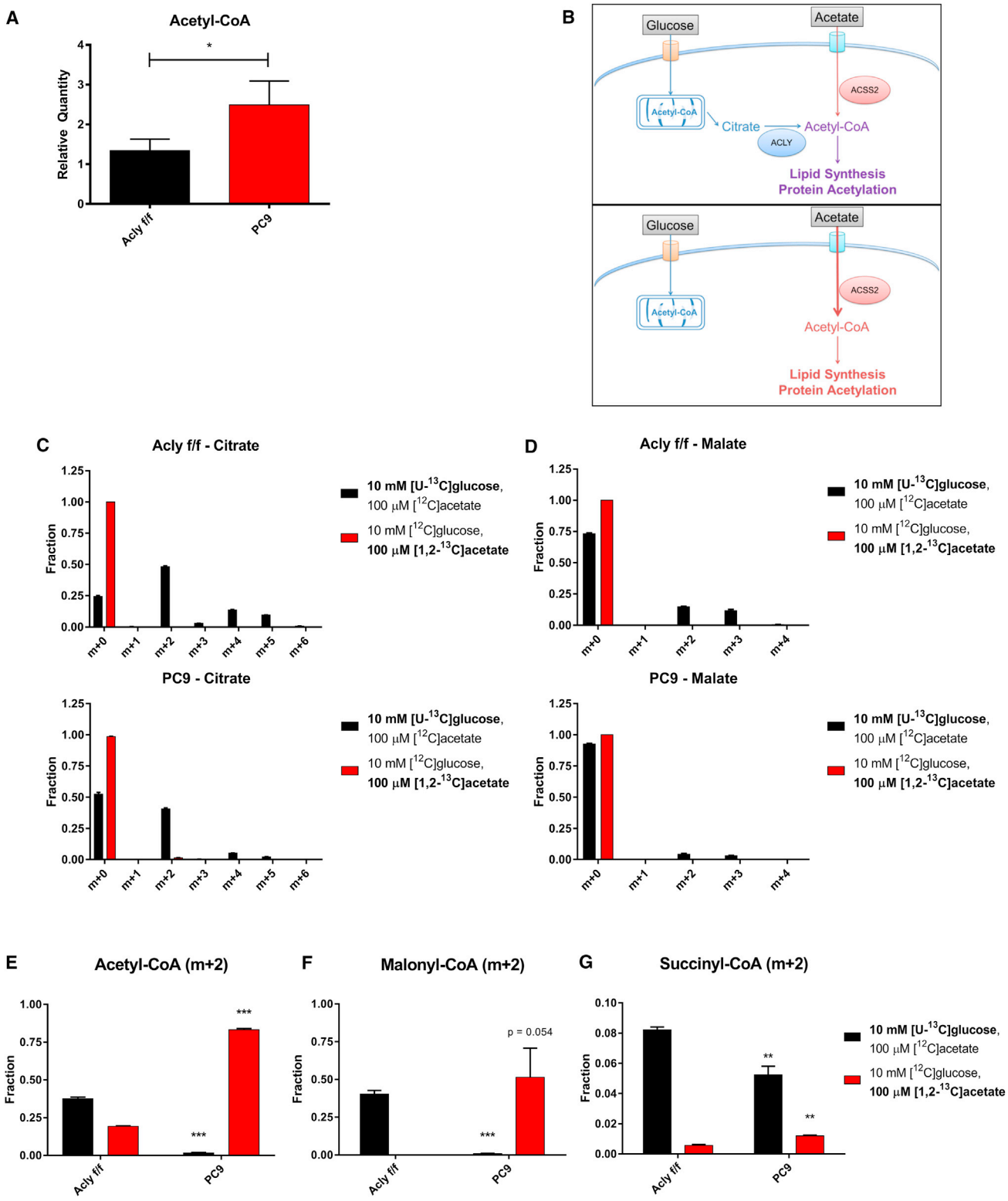

Figure 5. Acetyl-CoA Pools Are Sustained by Acetate in the Absence of ACLY

(A) Relative whole-cell acetyl-CoA levels in *Acly*$^{f/f}$ and PC9 MEFs cultured in glucose-free DMEM + 10% dFBS + 10 mM glucose + 100 μM sodium acetate for 6 hr, normalized to cellular volume; error bars indicate mean ± SD of triplicates.

(B) Schematic of acetyl-CoA production from glucose and acetate with (top) or without (bottom) ACLY.

(legend continued on next page)

in both VWAT and SWAT from *Acly*$^{FAT-/-}$ as compared to WT mice, while liver acetyl-CoA levels were slightly reduced (Figure 7A). To test whether *Acly*$^{FAT-/-}$ adipocytes supply acetyl-CoA and dependent biosynthetic processes using acetate, we isolated primary visceral adipocytes and tested acetate uptake. Indeed, acetyl-CoA, as well as malonyl-CoA and HMG-CoA, were more enriched from [1,2-^{13}C]acetate in primary adipocytes from *Acly*$^{FAT-/-}$ mice as compared to those from WT mice (Figures 7B–7D).

Next, we investigated the extent to which de novo synthesized fatty acids were present in adipose tissue in the absence of ACLY. To capture rates of de novo lipogenesis (DNL) in vivo, D_2O was administered to mice via a bolus injection and subsequent addition to drinking water for 3 weeks. At the conclusion of labeling VWAT, SWAT, and liver were collected, and total (saponified) fatty acids from each were analyzed by gas chromatography-mass spectrometry (GC-MS). Plasma D_2O enrichment was confirmed to be equivalent between genotypes (Figure S6A). In both VWAT and SWAT, abundance of the saturated fatty acids palmitic acid (C16:0) and stearic acid (C18:0) was significantly reduced (Figures S6B and S6C). Conversely, monounsaturated fatty acids, oleic acid (C18:1n9), and palmitoleic acid (C16:1n7), as well as the essential fatty acid linoleic acid (C18:2n6), were elevated in SWAT from *Acly*$^{FAT-/-}$ mice (Figure S6B). A slight reduction in palmitic acid was also observed in liver (Figure S6D). Fractional enrichment of fatty acids was not significantly different in VWAT between genotypes, although SWAT exhibited a moderate reduction in palmitic acid fractional synthesis (Figures S6E and S6F). Fractional synthesis was not different between genotypes in the liver, except for a small reduction for palmitoleic acid (Figure S6G).

The relative quantities of de novo synthesized fatty acids present in each tissue were calculated using plasma D_2O enrichment, fatty acid labeling, and abundance. Notably, DNL-derived fatty acids present in WAT may be synthesized in adipocytes or produced in the liver and transported to fat. In the SWAT of *Acly*$^{FAT-/-}$ mice, total de novo synthesized palmitic acid and stearic acid were significantly reduced (Figure 7E). In contrast, no significant differences in the quantities of DNL-generated fatty acids were detected between *Acly*$^{FAT-/-}$ and *Acly*$^{f/f}$ mice in VWAT (Figure 7F). Liver DNL was largely unchanged by adipocyte ACLY deficiency, although a slight reduction in palmitic acid synthesis was observed (Figure 7G). Since DNL-derived fatty acids were reduced in SWAT of *Acly*$^{FAT-/-}$ mice, this depot may maintain lipid droplet size through greater storage of diet-derived fatty acids, as suggested by elevated levels of linoleic acid (Figure S6B).

Histone acetylation levels were also analyzed. Despite ACSS2 upregulation and elevated acetyl-CoA levels, H3K9ac and H3K23ac were significantly lower, and H3K18ac trended lower, in the SWAT of *Acly*$^{FAT-/-}$ mice (Figure 7H). Interestingly, this difference was not observed in VWAT, suggesting that acetate compensation for ACLY deficiency may be more complete in this depot or that other factors are dominant in determining histone acetylation levels (Figure 7I). No differences in histone H3 acetylation were detected in the liver (Figure 7J). Altogether, the data suggest that, in vivo, adipocytes lacking ACLY partially compensate by engaging acetate metabolism.

DISCUSSION

The findings of this study demonstrate that ACLY is required for the vast majority of glucose-dependent fatty acid syntheses and histone acetylations under standard culture conditions and that ACSS2 upregulation and use of acetate carbon is a major mechanism of compensation for ACLY deficiency. Additionally, despite ACSS2 upregulation and higher acetyl-CoA levels, ACLY deficiency results in lower overall histone acetylation levels, slower proliferation, and altered gene expression patterns. The data suggest that ACLY and ACSS2 likely play distinct roles in the regulation of histone acetylation and gene expression but also indicate that the potential for metabolic compensation from acetate should be considered if ACLY is pursued as a therapeutic target.

From a clinical perspective, prior study of PET (positron emission tomography) imaging in human hepatocellular carcinoma patients using ^{11}C-acetate and ^{18}F-fluorodeoxyglucose (FDG) revealed a dichotomy between acetate and glucose uptake. Patient tumors, or regions within tumors, with high ^{11}C-acetate uptake demonstrated low ^{18}F-FDG uptake and vice versa. Moreover, tumors with high ^{18}F-FDG uptake were more proliferative (Yun et al., 2009). These data support the concept that mammalian cells—cancer cells, in particular—possess an intrinsic flexibility in their ability to acquire acetyl-CoA from different sources to adjust to changing metabolic environments in vivo. Further elucidation of the mechanisms connecting ACLY and ACSS2, as well as the differential phenotypes observed downstream of their activity, could point toward synthetic lethal strategies for cancer therapy or improved tumor imaging protocols.

In considering the roles of these enzymes in normal physiology, given the importance of GLUT4-dependent glucose uptake and glucose-dependent fatty acid synthesis for systemic metabolic homeostasis (Herman and Kahn, 2006; Herman et al., 2012), deletion of *Acly* in adipocytes results in a surprisingly mild phenotype, with no overt metabolic dysfunction observed for mixed-background mice on a regular chow diet. Nevertheless, larger adipocytes and reduced expression of genes, such as *Glut4*, observed in this model are also characteristic of obesity and are associated with poorer metabolic function. This suggests that *Acly*$^{FAT-/-}$ mice may be more susceptible to

(C) Isotopologue distribution of citrate after 6-hr incubation with 10 mM [U-^{13}C]glucose, with 100 μM unlabeled acetate present (black) or 100 μM [1,2-^{13}C]acetate with 10 mM unlabeled glucose present (red), in *Acly*$^{f/f}$ (top) or PC9 (bottom) MEFs; error bars indicate mean ± SEM of triplicates.
(D) Isotopologue distribution of malate in the same conditions as (C).
(E–G) m+2 acetyl-CoA (E), malonyl-CoA (F), or succinyl-CoA (G) following 6-hr labeling in 10 mM [U-^{13}C]glucose (with 100 μM unlabeled acetate present) or 100 μM [1,2-^{13}C]acetate (with 10 mM unlabeled glucose present); error bars indicate mean ± SEM of triplicates. For (E–G), all statistical comparisons are to *Acly*$^{f/f}$ using Holm-Sidak test.
For all panels: *$p < 0.05$; **$p < 0.01$; ***$p < 0.001$.
See also Figure S5.

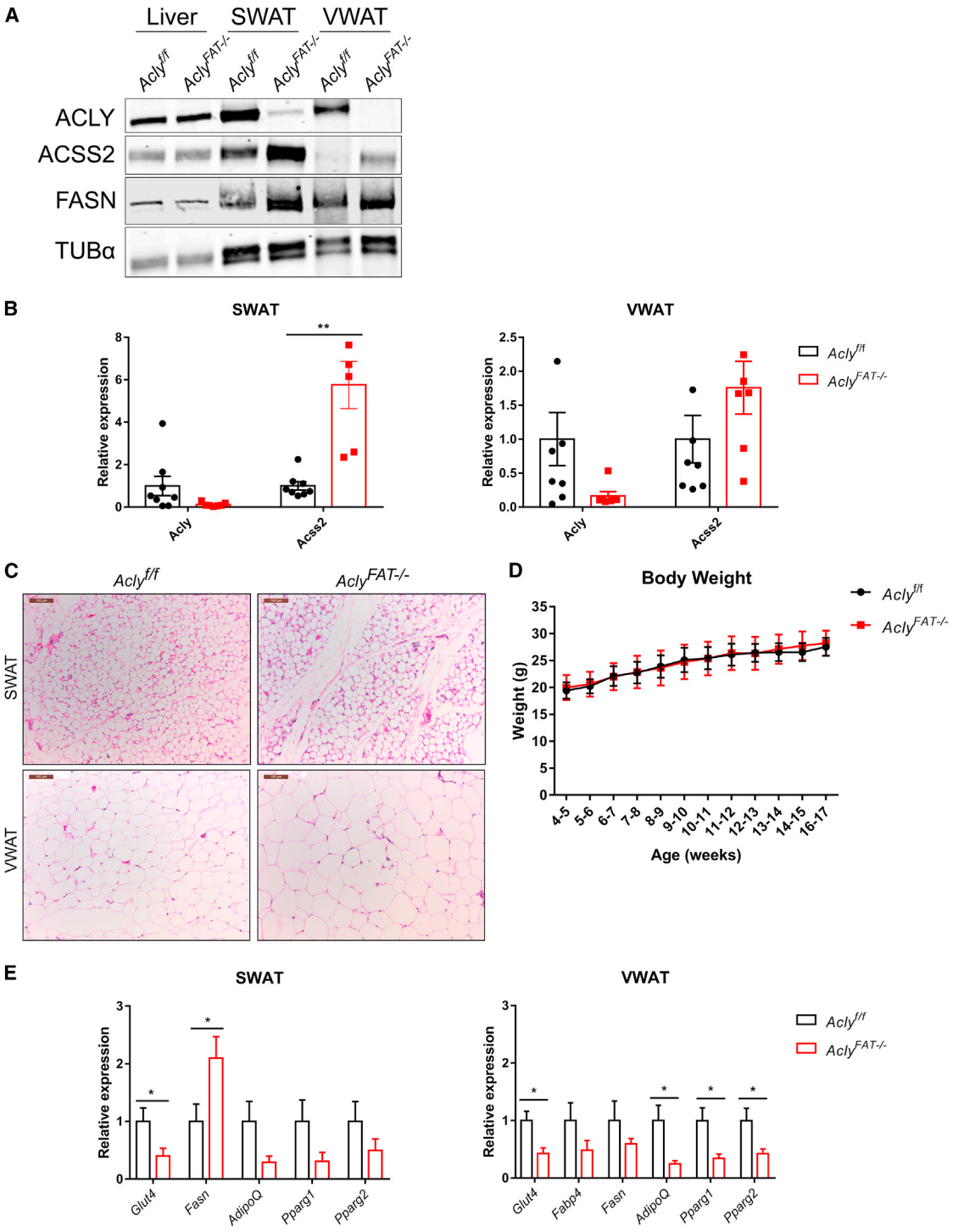

Figure 6. ACSS2 Is Upregulated In Vivo upon Deletion of *Acly* from Adipocytes

(A) Western blot of liver, SWAT, and VWAT from *Acly*$^{f/f}$ and *Acly*$^{FAT-/-}$ mice.

(B) mRNA expression of *Acly* and *Acss2* in SWAT (left) and VWAT (right) from *Acly*$^{f/f}$ and *Acly*$^{FAT-/-}$ mice; error bars indicate mean ± SEM.

(C) Representative SWAT and VWAT histology from male 16-week-old *Acly*$^{f/f}$ and *Acly*$^{FAT-/-}$ mice. Scale bars, 100 μm.

(D) Body weight of male *Acly*$^{f/f}$ (n = 9) and *Acly*$^{FAT-/-}$ (n = 8) mice; error bars indicate mean ± SD.

(E) Expression of adipocyte genes in SWAT (left) and VWAT (right) from *Acly*$^{f/f}$ (n = 8) and *Acly*$^{FAT-/-}$ (n = 7) mice; error bars indicate mean ± SEM.

For all panels: *p < 0.05; **p < 0.01.

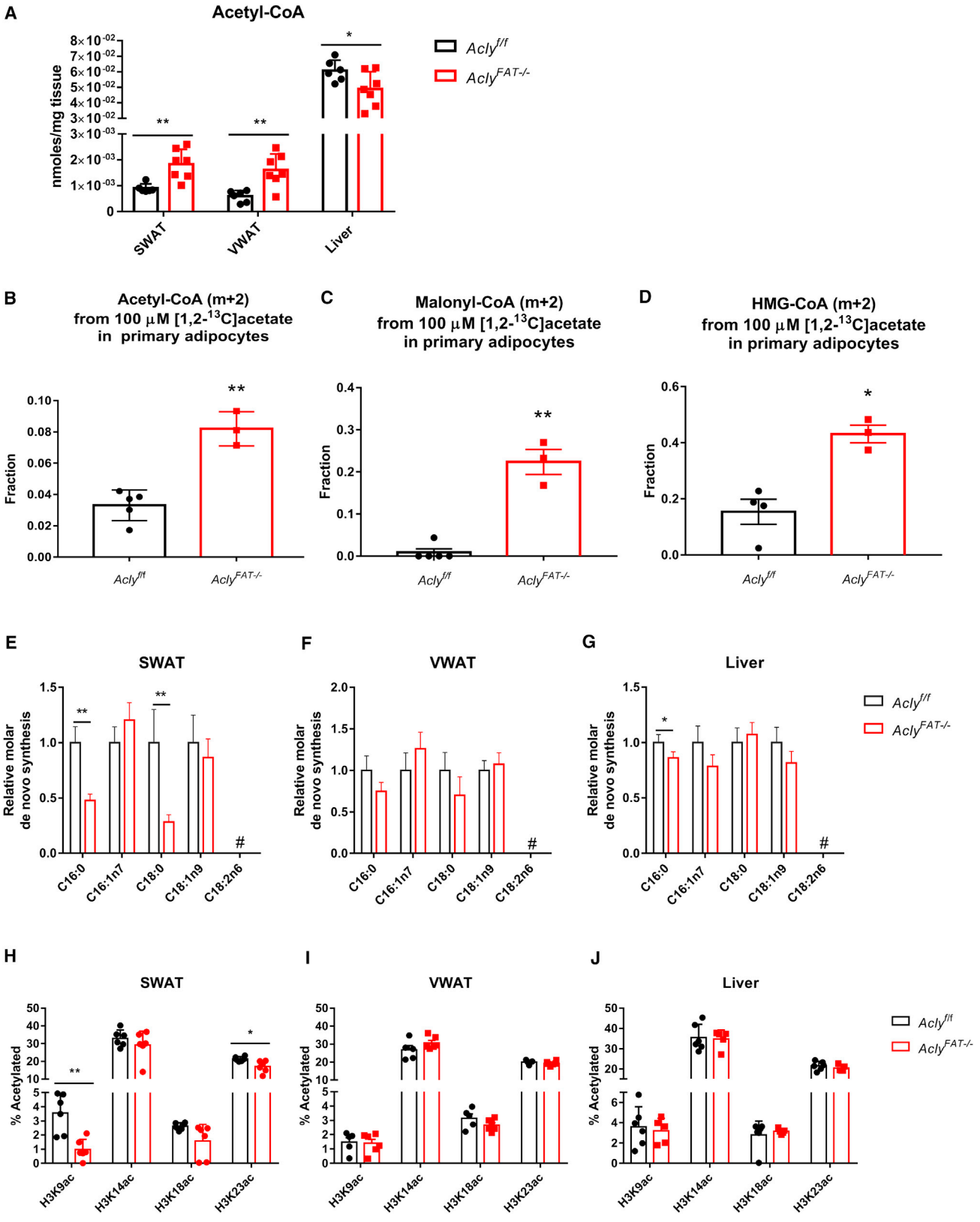

(legend on next page)

metabolic dysfunction when nutritionally stressed, for example, with high fructose feeding. Another interesting question is whether these mice will exhibit exacerbated metabolic phenotypes under conditions that alter acetate availability in the bloodstream, such as ethanol consumption or antibiotic treatment.

The differential impact of ACLY on SWAT and VWAT also warrants further investigation. It is not clear why SWAT, but not VWAT, exhibits reduced histone acetylation and de novo fatty acid synthesis, despite evidence for compensatory mechanisms such as FASN upregulation. One possible explanation relates to an overall greater fraction of fatty acids that are de novo synthesized in SWAT, as compared to VWAT (Figures S6E and S6F), placing a greater demand for acetyl-CoA. Potentially, in a tissue with a lower DNL rate, acetate may be more readily able to compensate in both DNL and histone acetylation. Distribution of fatty acids in $Acly^{FAT-/-}$ WAT depots is also altered; SWAT, in particular, exhibits increased levels of monounsaturated and essential fatty acids (Figure S6B). Palmitoleate, which has been implicated as an insulin-sensitizing lipokine (Cao et al., 2008), is elevated in ACLY-deficient SWAT, raising questions about how altered levels of bioactive lipid species in the absence of ACLY may influence metabolic phenotypes. More mechanistic work is also clearly needed to elucidate the relationship between ACLY and gene regulation. The relationship between global histone acetylation and gene expression is not entirely consistent between VWAT and SWAT, possibly reflecting gene regulatory mechanisms that are specific to ACLY.

A noteworthy observation in this study is that acetyl-CoA and histone acetylation levels appear to become uncoupled in the absence of ACLY, suggesting that acetate-derived acetyl-CoA may not be efficiently used for histone acetylation. Several possible mechanisms could account for this. First, it may be that, in MEFs, an insufficient amount of ACSS2 is present in the nucleus to efficiently drive histone acetylation. ACSS2 has been found to localize prominently to the nucleus in some conditions (Chen et al., 2015; Comerford et al., 2014; Xu et al., 2014); thus, investigation of whether acetate more readily contributes to overall histone acetylation levels in these contexts will be informative. However, potentially arguing against this possibility, hypoxia promotes ACSS2 nuclear localization (Xu et al., 2014); yet, although acetate does regulate histone acetylation in hypoxic cells, a high level of acetate (~2.5 mM) is required (Gao et al., 2016). A second possibility is that, within the nucleus, acetyl-CoA producing enzymes are channeled, compartmentalized into niches, or sequestered with particular binding partners. Through such a mechanism, acetylation of specific proteins may be regulated not only by the relevant acetyltransferase but also by a specific acetyl-CoA-producing enzyme. Consistent with this possibility, acetylation of HIF2α was shown to be exclusively dependent on ACSS2 as a source of acetyl-CoA (Chen et al., 2015; Xu et al., 2014). A third possibility is that ACLY-deficient conditions may result in altered lysine acetyltransferase (KAT) or HDAC (histone deacetylase) activity. Finally, a fourth possibility is that lower use of acetyl-CoA for histone acetylation could be a feature of slow proliferation in the absence of ACLY (i.e., secondary to the proliferation defect). However, prior findings that histone acetylation is sensitive to glucose availability over a range that did not impact proliferation (Lee et al., 2014) and that the TCA cycle (which supplies ACLY substrate citrate) and mitochondrial membrane potential have distinct and separate roles in regulating histone acetylation and proliferation, respectively (Martínez-Reyes et al., 2016), as well as data in the present article showing that histone acetylation can be boosted by high acetate without a corresponding rescue of proliferation, argue against this as a sole explanation. Nevertheless, elucidation of the mechanisms that constrain proliferation in the absence of ACLY could help to definitively address this.

Investigating these possibilities will illuminate whether cells possess mechanisms to differentially detect ACLY-generated versus ACSS2-generated acetyl-CoA as well as define the functional relationship between histone acetylation levels and cellular functions and phenotypes. Given that ACLY dominates in nutrient- and oxygen-replete conditions, whereas ACSS2 becomes important in nutrient- and oxygen-poor conditions (Gao et al., 2016; Schug et al., 2015), having mechanisms such as different acetylation substrates to distinguish between acetyl-CoA produced by each enzyme could be advantageous to cells. For example, such mechanisms could potentially cue cells to grow when ACLY serves as the acetyl-CoA source and to mediate adaptive responses when ACSS2 is the primary acetyl-CoA source. The roles of these enzymes in gene regulation appear to be complex, and in-depth analysis of the respective roles of ACLY and ACSS2 in genome-wide histone acetylation and acetylation of other protein substrates is needed to begin addressing these questions.

Recent work has shown that the PDC is present in the nucleus and is able to convert pyruvate to acetyl-CoA for use in histone acetylation (Sutendra et al., 2014), raising the question of how the findings of the present study can be aligned with the described role of nuclear PDC. We suggest two potential models that are consistent both with our data and with a role for nuclear PDC in histone acetylation. In the first model,

Figure 7. ACLY-Deficient Adipose Tissue Exhibits Depot-Specific Alterations in DNL and Histone Acetylation

(A) Acetyl-CoA abundance in SWAT, VWAT, and liver in 11-week-old $Acly^{f/f}$ (n = 6) and $Acly^{FAT-/-}$ (n = 7) mice.

(B–D) Primary mature adipocytes were isolated from 12- to 16-week-old $Acly^{f/f}$ (n = 5) and $Acly^{FAT-/-}$ (n = 3) mice and labeled with 100 μM [1,2-^{13}C]acetate (with 5 mM unlabeled glucose present). Acetyl-CoA (B), malonyl-CoA (C), and HMG-CoA (D) enrichment from acetate was analyzed; error bars indicate mean ± SEM.

(E–G) Relative quantities of fatty acids synthesized de novo in SWAT (E), VWAT (F), and liver (G) of $Acly^{f/f}$ (n = 6) and $Acly^{FAT-/-}$ (n = 8) mice; error bars indicate mean ± SEM. The # sign indicates not synthesized de novo.

(H–J) Overall histone H3 acetylation levels in 11-week-old SWAT (H), VWAT (I), and liver (J) of $Acly^{f/f}$ (n = 6) and $Acly^{FAT-/-}$ (n = 7) mice; error bars indicate mean ± SEM.

For all panels: *$p < 0.05$; **$p < 0.01$.

See also Figure S6.

ACLY is the primary acetyl-CoA producer for regulation of global levels of histone acetylation, while PDC (and, potentially, other nuclear acetyl-CoA sources such as CrAT) could participate in mediating histone acetylation at specific target genes but not globally. A recent report that PDC forms a complex with PKM2, p300, and the arylhydrocarbon receptor (AhR) to facilitate histone acetylation at AhR target genes is consistent with such a possibility (Matsuda et al., 2015). In the second model, the role of ACLY in glucose-dependent histone acetylation regulation could be context dependent, with a larger role for PDC emerging in certain conditions or cell types. This possibility is supported by observations that PDC nuclear translocation is stimulated by conditions such as growth factor stimulation and mitochondrial stress (Sutendra et al., 2014). Further investigation will be needed to evaluate these models.

In sum, this study points to a crucial interplay between glucose and acetate metabolism to supply the nuclear-cytosolic acetyl-CoA pool for fatty acid synthesis and histone acetylation. At the same time, it shows that, despite compensatory mechanisms, ACLY is required for optimal proliferation, and simply increasing nuclear-cytosolic acetyl-CoA production is insufficient to fully replace ACLY. This could point to the importance of ACLY's other product, oxaloacetate; a build-up of ACLY's substrate citrate; deficiencies in anapleurosis and/or mitochondrial function upon loss of a major catapleurotic pathway; or a signaling mechanism that is specific to ACLY. Clearly, more work is needed both to understand the mechanisms through which ACLY facilitates cell proliferation and to further define the ways that cells partition and use acetyl-CoA produced by different enzymes. The findings of this study raise a number of important questions for future investigation, as discussed earlier. They also clarify the importance of ACLY in glucose-dependent acetyl-CoA production outside of mitochondria and provide key insights into the mechanisms of metabolic flexibility used for production of nuclear-cytosolic acetyl-CoA. Understanding these compensatory mechanisms will be important to consider for therapeutic targeting of acetyl-CoA metabolic pathways.

EXPERIMENTAL PROCEDURES

Generation of *Acly*$^{f/f}$ and *Acly*$^{FAT-/-}$ Mice

A Knockout First targeting vector was obtained from the Knockout Mouse Project (KOMP) that targets exon 9 of Acly (KOMP: 80097), predicted to result in a truncated protein subject to nonsense-mediated decay. The Knockout First allele is initially null but can be converted to a conditional floxed allele upon Flp recombination (Skarnes et al., 2011). Recombinant 129/B6 hybrid embryonic stem cells (ESCs) were generated in Penn's Gene Targeting Core, and blastocysts were injected at Penn's Transgenic and Chimeric Mouse Core. Upon acquisition of the chimeric mice, animals were bred to obtain germline transmission. *Acly*$^{f/+}$ progenies were selected through sequential breeding with wild-type C57Bl/6J mice (purchased from Jackson Laboratory) and mice expressing Flp recombinase (B6.Cg-Tg(ACTFLPe)9205Dym/J, Jackson Laboratory). Finally, *Acly*$^{f/f}$ mice were generated by interbreeding and selected by genotyping (see the Supplemental Information). Immortalized *Acly*$^{f/f}$ MEFs were generated from these mice (see the Supplemental Information). To produce *Acly*$^{FAT-/-}$ mice, *Acly*$^{f/f}$ mice were bred to adiponectin-Cre transgenic mice (stock no: 010803; B6;FVB-Tg(Adipoq-cre)1Evdr/J, Jackson Laboratory). The University of Pennsylvania's Institutional Animal Care and Use Committee (IACUC) approved all animal experiments.

In Vivo De Novo Lipogenesis

13-week-old male Acly$^{f/f}$ (n = 6) and Acly$^{FAT-/-}$ (n = 7) mice (C57Bl/6 backcrossed) were injected intraperitoneally (i.p.) with 0.035 mL/g of body weight of 0.9% NaCl D_2O (Sigma-Aldrich). For 3 subsequent weeks, mice were provided water bottles containing 8% D_2O. At the end of 3 weeks, mice were fasted for 6 hr and sacrificed, and plasma, liver, VWAT, and SWAT were collected and snap frozen. Plasma from four additional mice (two *Acly*$^{f/f}$ and two *Acly*$^{FAT-/-}$) that were not given D_2O was used as controls. See the Supplemental Information for details of analysis.

Cell Culture and Proliferation Assays

MEFs (generation described in the Supplemental Information) were cultured in DMEM (GIBCO) supplemented with 10% Cosmic Calf Serum (CS) (HyClone, SH30087.03, lot number AXA30096). LN229 cells were cultured in RPMI 1640 medium (GIBCO) supplemented with 10% CS (HyClone SH30087.03, lot number AXA30096) and 2 mM L-glutamine. For experiments using dFBS, cells were cultured in glucose-free DMEM + 10% dFBS (GIBCO 26400044), with indicated concentrations of glucose and sodium acetate added. For proliferation assays, cells were plated in triplicate at the indicated density and allowed to adhere overnight. Culture medium was changed the following day, and cells were allowed to proliferate until the indicated days following plating. Cells were collected and counted on a hemocytometer. Cell lines used for viral production included Phoenix E and HEK293T cells, which were purchased from ATCC. Cells were cultured in DMEM + 10% CS and used at low passage. All cell lines were routinely monitored and confirmed to be free of mycoplasma.

Acyl-CoA Quantification and Isotopologue Analysis

Acyl-CoA species were extracted in 1 mL 10% (w/v) trichloroacetic acid (Sigma-Aldrich, catalog #T6399). Isotopologue enrichment analysis to quantify the incorporation of 10 mM [U-^{13}C]glucose and 100 μM [U-^{13}C]acetate into acyl-CoA thioesters was performed by liquid chromatograpy-mass spectrometry/high-resolution mass spectrometry (LC-MS/HRMS). For quantitation, internal standards containing [$^{13}C_3{}^{15}N_1$]-labeled acyl-CoAs generated in *pan6*-deficient yeast culture (Snyder et al., 2015) were added to each sample in equal amounts. Samples were analyzed by an Ultimate 3000 autosampler coupled to a Thermo Q Exactive Plus instrument in positive electrospray ionization (ESI) mode using the settings described previously (Frey et al., 2016). A more detailed method can be found in the Supplemental Information.

Statistics

Student's two-tailed t tests (two-sample equal variance, two-tailed distribution) were used for analyses directly comparing two datasets except tissue gene expression and acyl-CoA datasets (Figures 6 and 7), for which Welch's t test was used. Significance was defined as follows: *p < 0.05; **p < 0.01; ***p < 0.001; and ****p < 0.0001.

Please also see the Supplemental Experimental Procedures.

SUPPLEMENTAL INFORMATION

Supplemental Information includes Supplemental Experimental Procedures and six figures and can be found with this article online at http://dx.doi.org/10.1016/j.celrep.2016.09.069.

AUTHOR CONTRIBUTIONS

The project was conceptualized and designed by S.Z. and K.E.W. S.Z. performed the majority of cell culture experiments and GC-MS metabolite analysis. A.T. generated *Acly*$^{FAT-/-}$ mice and performed the majority of animal experiments. R.A.H., Y.-M.K., and A.J.A. conducted mass spectrometry analysis of histone acetylation. S.T., A.J.F., I.A.B., and N.W.S. conducted acyl-CoA measurements by LC-MS. J.V.L., S.L.C., and J.M.V. conducted experiments. A.C. generated *Acly*$^{f/f}$ MEFs and assisted with mouse experiments. A.S. and A.M.W. conducted NMR acetate measurements. M.W., N.M., and C.M.M. analyzed tissue rates of DNL from D_2O-labeled mice. S.Z. and A.M.T. prepared

figures. K.E.W. guided the study, analyzed data, and wrote the manuscript. All authors read and provided feedback on manuscript and figures.

ACKNOWLEDGMENTS

This work was supported by grant R01CA174761, a Pew Biomedical Scholar Award, an American Diabetes Association Junior Faculty Award (7-12-JF-59), and the Linda Pechenik Montague Investigator Award to K.E.W. S.Z. is supported by predoctoral training grant 5T32CA115299. A.T. is supported by Penn-PORT IRACDA postdoctoral fellowship K12 GM081259. J.V.L. is supported by predoctoral fellowship F31 CA189744. I.A.B. is supported by NIH grant P30ES013508. K.E.W. and I.A.B. also acknowledge support from the Abramson Cancer Center Basic Science Center of Excellence in Cancer Metabolism. A.J.A. is supported by NIH grant GM102503. N.W.S. is supported by grants K22ES26235 and R21HD087866. C.M.M. acknowledges grant R01CA188652. We thank Tobias Raabe from the Penn Gene Targeting Core and Jean Richa from the Transgenic and Chimeric Mouse Core for generation of the embryonic stem cells and chimeric mice that were used to produce the *Acly*$^{f/f}$ mice. We thank Tony Mancuso from the AFCRI Quantitative Metabolomics Core for guidance on GC-MS metabolite analysis. We thank James Alwine, Chi Dang, and K.E.W. lab members for helpful discussions during the preparation of this manuscript.

Received: April 12, 2016
Revised: August 9, 2016
Accepted: September 21, 2016
Published: October 18, 2016

REFERENCES

Ballantyne, C.M., Davidson, M.H., Macdougall, D.E., Bays, H.E., Dicarlo, L.A., Rosenberg, N.L., Margulies, J., and Newton, R.S. (2013). Efficacy and safety of a novel dual modulator of adenosine triphosphate-citrate lyase and adenosine monophosphate-activated protein kinase in patients with hypercholesterolemia: results of a multicenter, randomized, double-blind, placebo-controlled, parallel-group trial. J. Am. Coll. Cardiol. *62*, 1154–1162.

Balmer, M.L., Ma, E.H., Bantug, G.R., Grählert, J., Pfister, S., Glatter, T., Jauch, A., Dimeloe, S., Slack, E., Dehio, P., et al. (2016). Memory CD8(+) T cells require increased concentrations of acetate induced by stress for optimal function. Immunity *44*, 1312–1324.

Bauer, D.E., Hatzivassiliou, G., Zhao, F., Andreadis, C., and Thompson, C.B. (2005). ATP citrate lyase is an important component of cell growth and transformation. Oncogene *24*, 6314–6322.

Beigneux, A.P., Kosinski, C., Gavino, B., Horton, J.D., Skarnes, W.C., and Young, S.G. (2004). ATP-citrate lyase deficiency in the mouse. J. Biol. Chem. *279*, 9557–9564.

Cai, L., Sutter, B.M., Li, B., and Tu, B.P. (2011). Acetyl-CoA induces cell growth and proliferation by promoting the acetylation of histones at growth genes. Mol. Cell *42*, 426–437.

Cao, H., Gerhold, K., Mayers, J.R., Wiest, M.M., Watkins, S.M., and Hotamisligil, G.S. (2008). Identification of a lipokine, a lipid hormone linking adipose tissue to systemic metabolism. Cell *134*, 933–944.

Carrer, A., and Wellen, K.E. (2015). Metabolism and epigenetics: a link cancer cells exploit. Curr. Opin. Biotechnol. *34*, 23–29.

Chen, R., Xu, M., Nagati, J.S., Hogg, R.T., Das, A., Gerard, R.D., and Garcia, J.A. (2015). The acetate/ACSS2 switch regulates HIF-2 stress signaling in the tumor cell microenvironment. PLoS ONE *10*, e0116515.

Chen, W.W., Freinkman, E., Wang, T., Birsoy, K., and Sabatini, D.M. (2016). Absolute quantification of matrix metabolites reveals the dynamics of mitochondrial metabolism. Cell *166*, 1324–1337.e11.

Cluntun, A.A., Huang, H., Dai, L., Liu, X., Zhao, Y., and Locasale, J.W. (2015). The rate of glycolysis quantitatively mediates specific histone acetylation sites. Cancer Metab. *3*, 10.

Comerford, S.A., Huang, Z., Du, X., Wang, Y., Cai, L., Witkiewicz, A.K., Walters, H., Tantawy, M.N., Fu, A., Manning, H.C., et al. (2014). Acetate dependence of tumors. Cell *159*, 1591–1602.

Covarrubias, A.J., Aksoylar, H.I., Yu, J., Snyder, N.W., Worth, A.J., Iyer, S.S., Wang, J., Ben-Sahra, I., Byles, V., Polynne-Stapornkul, T., et al. (2016). Akt-mTORC1 signaling regulates Acly to integrate metabolic input to control of macrophage activation. eLife *5*, e11612.

Donohoe, D.R., Collins, L.B., Wali, A., Bigler, R., Sun, W., and Bultman, S.J. (2012). The Warburg effect dictates the mechanism of butyrate-mediated histone acetylation and cell proliferation. Mol. Cell *48*, 612–626.

Frey, A.J., Feldman, D.R., Trefely, S., Worth, A.J., Basu, S.S., and Snyder, N.W. (2016). LC-quadrupole/Orbitrap high-resolution mass spectrometry enables stable isotope-resolved simultaneous quantification and ^{13}C-isotopic labeling of acyl-coenzyme A thioesters. Anal. Bioanal. Chem. *408*, 3651–3658.

Gao, X., Lin, S.H., Ren, F., Li, J.T., Chen, J.J., Yao, C.B., Yang, H.B., Jiang, S.X., Yan, G.Q., Wang, D., et al. (2016). Acetate functions as an epigenetic metabolite to promote lipid synthesis under hypoxia. Nat. Commun. *7*, 11960.

Gutierrez, M.J., Rosenberg, N.L., Macdougall, D.E., Hanselman, J.C., Margulies, J.R., Strange, P., Milad, M.A., McBride, S.J., and Newton, R.S. (2014). Efficacy and safety of ETC-1002, a novel investigational low-density lipoprotein-cholesterol-lowering therapy for the treatment of patients with hypercholesterolemia and type 2 diabetes mellitus. Arterioscler. Thromb. Vasc. Biol. *34*, 676–683.

Hanai, J., Doro, N., Sasaki, A.T., Kobayashi, S., Cantley, L.C., Seth, P., and Sukhatme, V.P. (2012). Inhibition of lung cancer growth: ATP citrate lyase knockdown and statin treatment leads to dual blockade of mitogen-activated protein kinase (MAPK) and phosphatidylinositol-3-kinase (PI3K)/AKT pathways. J. Cell. Physiol. *227*, 1709–1720.

Hanai, J.I., Doro, N., Seth, P., and Sukhatme, V.P. (2013). ATP citrate lyase knockdown impacts cancer stem cells in vitro. Cell Death Dis. *4*, e696.

Hatzivassiliou, G., Zhao, F., Bauer, D.E., Andreadis, C., Shaw, A.N., Dhanak, D., Hingorani, S.R., Tuveson, D.A., and Thompson, C.B. (2005). ATP citrate lyase inhibition can suppress tumor cell growth. Cancer Cell *8*, 311–321.

Herman, M.A., and Kahn, B.B. (2006). Glucose transport and sensing in the maintenance of glucose homeostasis and metabolic harmony. J. Clin. Invest. *116*, 1767–1775.

Herman, M.A., Peroni, O.D., Villoria, J., Schön, M.R., Abumrad, N.A., Blüher, M., Klein, S., and Kahn, B.B. (2012). A novel ChREBP isoform in adipose tissue regulates systemic glucose metabolism. Nature *484*, 333–338.

Herrmann, D.B., Herz, R., and Fröhlich, J. (1985). Role of gastrointestinal tract and liver in acetate metabolism in rat and man. Eur. J. Clin. Invest. *15*, 221–226.

Kamphorst, J.J., Chung, M.K., Fan, J., and Rabinowitz, J.D. (2014). Quantitative analysis of acetyl-CoA production in hypoxic cancer cells reveals substantial contribution from acetate. Cancer Metab. *2*, 23.

Lee, K.Y., Russell, S.J., Ussar, S., Boucher, J., Vernochet, C., Mori, M.A., Smyth, G., Rourk, M., Cederquist, C., Rosen, E.D., et al. (2013). Lessons on conditional gene targeting in mouse adipose tissue. Diabetes *62*, 864–874.

Lee, J.V., Carrer, A., Shah, S., Snyder, N.W., Wei, S., Venneti, S., Worth, A.J., Yuan, Z.F., Lim, H.W., Liu, S., et al. (2014). Akt-dependent metabolic reprogramming regulates tumor cell histone acetylation. Cell Metab. *20*, 306–319.

Lee, J.H., Jang, H., Lee, S.M., Lee, J.E., Choi, J., Kim, T.W., Cho, E.J., and Youn, H.D. (2015). ATP-citrate lyase regulates cellular senescence via an AMPK- and p53-dependent pathway. FEBS J. *282*, 361–371.

Lundquist, F., Tygstrup, N., Winkler, K., Mellemgaard, K., and Munck-Petersen, S. (1962). Ethanol metabolism and production of free acetate in the human liver. J. Clin. Invest. *41*, 955–961.

Luong, A., Hannah, V.C., Brown, M.S., and Goldstein, J.L. (2000). Molecular characterization of human acetyl-CoA synthetase, an enzyme regulated by sterol regulatory element-binding proteins. J. Biol. Chem. *275*, 26458–26466.

Madiraju, P., Pande, S.V., Prentki, M., and Madiraju, S.R. (2009). Mitochondrial acetylcarnitine provides acetyl groups for nuclear histone acetylation. Epigenetics *4*, 399–403.

Martínez-Reyes, I., Diebold, L.P., Kong, H., Schieber, M., Huang, H., Hensley, C.T., Mehta, M.M., Wang, T., Santos, J.H., Woychik, R., et al. (2016). TCA cycle and mitochondrial membrane potential are necessary for diverse biological functions. Mol. Cell *61*, 199–209.

Mashimo, T., Pichumani, K., Vemireddy, V., Hatanpaa, K.J., Singh, D.K., Sirasanagandla, S., Nannepaga, S., Piccirillo, S.G., Kovacs, Z., Foong, C., et al. (2014). Acetate is a bioenergetic substrate for human glioblastoma and brain metastases. Cell *159*, 1603–1614.

Matsuda, S., Adachi, J., Ihara, M., Tanuma, N., Shima, H., Kakizuka, A., Ikura, M., Ikura, T., and Matsuda, T. (2015). Nuclear pyruvate kinase M2 complex serves as a transcriptional coactivator of arylhydrocarbon receptor. Nucleic Acids Res. *44*, 636–647.

McBrian, M.A., Behbahan, I.S., Ferrari, R., Su, T., Huang, T.W., Li, K., Hong, C.S., Christofk, H.R., Vogelauer, M., Seligson, D.B., and Kurdistani, S.K. (2013). Histone acetylation regulates intracellular pH. Mol. Cell *49*, 310–321.

Migita, T., Narita, T., Nomura, K., Miyagi, E., Inazuka, F., Matsuura, M., Ushijima, M., Mashima, T., Seimiya, H., Satoh, Y., et al. (2008). ATP citrate lyase: activation and therapeutic implications in non-small cell lung cancer. Cancer Res. *68*, 8547–8554.

Pearce, N.J., Yates, J.W., Berkhout, T.A., Jackson, B., Tew, D., Boyd, H., Camilleri, P., Sweeney, P., Gribble, A.D., Shaw, A., and Groot, P.H. (1998). The role of ATP citrate-lyase in the metabolic regulation of plasma lipids. Hypolipidaemic effects of SB-204990, a lactone prodrug of the potent ATP citrate-lyase inhibitor SB-201076. Biochem. J. *334*, 113–119.

Perry, R.J., Peng, L., Barry, N.A., Cline, G.W., Zhang, D., Cardone, R.L., Petersen, K.F., Kibbey, R.G., Goodman, A.L., and Shulman, G.I. (2016). Acetate mediates a microbiome-brain-β-cell axis to promote metabolic syndrome. Nature *534*, 213–217.

Pietrocola, F., Galluzzi, L., Bravo-San Pedro, J.M., Madeo, F., and Kroemer, G. (2015). Acetyl coenzyme A: a central metabolite and second messenger. Cell Metab. *21*, 805–821.

Scheppach, W., Pomare, E.W., Elia, M., and Cummings, J.H. (1991). The contribution of the large intestine to blood acetate in man. Clin. Sci. *80*, 177–182.

Schug, Z.T., Peck, B., Jones, D.T., Zhang, Q., Grosskurth, S., Alam, I.S., Goodwin, L.M., Smethurst, E., Mason, S., Blyth, K., et al. (2015). Acetyl-CoA synthetase 2 promotes acetate utilization and maintains cancer cell growth under metabolic stress. Cancer Cell *27*, 57–71.

Schug, Z.T., Vande Voorde, J., and Gottlieb, E. (2016). The metabolic fate of acetate in cancer. Nat. Rev. Cancer. http://dx.doi.org/10.1038/nrc.2016.87.

Shah, S., Carriveau, W.J., Li, J., Campbell, S.L., Kopinski, P.K., Lim, H.W., Daurio, N., Trefely, S., Won, K.J., Wallace, D.C., et al. (2016). Targeting ACLY sensitizes castration-resistant prostate cancer cells to AR antagonism by impinging on an ACLY-AMPK-AR feedback mechanism. Oncotarget. http://dx.doi.org/10.18632/oncotarget.9666.

Skarnes, W.C., Rosen, B., West, A.P., Koutsourakis, M., Bushell, W., Iyer, V., Mujica, A.O., Thomas, M., Harrow, J., Cox, T., et al. (2011). A conditional knockout resource for the genome-wide study of mouse gene function. Nature *474*, 337–342.

Skutches, C.L., Holroyde, C.P., Myers, R.N., Paul, P., and Reichard, G.A. (1979). Plasma acetate turnover and oxidation. J. Clin. Invest. *64*, 708–713.

Snyder, N.W., Tombline, G., Worth, A.J., Parry, R.C., Silvers, J.A., Gillespie, K.P., Basu, S.S., Millen, J., Goldfarb, D.S., and Blair, I.A. (2015). Production of stable isotope-labeled acyl-coenzyme A thioesters by yeast stable isotope labeling by essential nutrients in cell culture. Anal. Biochem. *474*, 59–65.

Sutendra, G., Kinnaird, A., Dromparis, P., Paulin, R., Stenson, T.H., Haromy, A., Hashimoto, K., Zhang, N., Flaim, E., and Michelakis, E.D. (2014). A nuclear pyruvate dehydrogenase complex is important for the generation of acetyl-CoA and histone acetylation. Cell *158*, 84–97.

Takahashi, H., McCaffery, J.M., Irizarry, R.A., and Boeke, J.D. (2006). Nucleocytosolic acetyl-coenzyme a synthetase is required for histone acetylation and global transcription. Mol. Cell *23*, 207–217.

Tollinger, C.D., Vreman, H.J., and Weiner, M.W. (1979). Measurement of acetate in human blood by gas chromatography: effects of sample preparation, feeding, and various diseases. Clin. Chem. *25*, 1787–1790.

Wellen, K.E., Hatzivassiliou, G., Sachdeva, U.M., Bui, T.V., Cross, J.R., and Thompson, C.B. (2009). ATP-citrate lyase links cellular metabolism to histone acetylation. Science *324*, 1076–1080.

Xu, M., Nagati, J.S., Xie, J., Li, J., Walters, H., Moon, Y.A., Gerard, R.D., Huang, C.L., Comerford, S.A., Hammer, R.E., et al. (2014). An acetate switch regulates stress erythropoiesis. Nat. Med. *20*, 1018–1026.

Yoshii, Y., Waki, A., Furukawa, T., Kiyono, Y., Mori, T., Yoshii, H., Kudo, T., Okazawa, H., Welch, M.J., and Fujibayashi, Y. (2009). Tumor uptake of radiolabeled acetate reflects the expression of cytosolic acetyl-CoA synthetase: implications for the mechanism of acetate PET. Nucl. Med. Biol. *36*, 771–777.

Yun, M., Bang, S.H., Kim, J.W., Park, J.Y., Kim, K.S., and Lee, J.D. (2009). The importance of acetyl coenzyme A synthetase for 11C-acetate uptake and cell survival in hepatocellular carcinoma. J. Nucl. Med. *50*, 1222–1228.

Zaidi, N., Royaux, I., Swinnen, J.V., and Smans, K. (2012). ATP citrate lyase knockdown induces growth arrest and apoptosis through different cell- and environment-dependent mechanisms. Mol. Cancer Ther. *11*, 1925–1935.